JOURNAL OF MATERIALS SCIENCE **35** (2000) 2993–3001

Vibrational properties of wood along the grain

E. OBATAYA
Institute of Agricultural and Forest Engineering, Univerisity of Tsukuba, Ibaraki, 305-8572, Japan
E-mail: obataya@agbi.tsukuba.ac.jp

T. ONO
Faculty of Engineering, Gifu University, Gifu, 501-1112, Japan

M. NORIMOTO
Wood Research Institute, Kyoto University, Uji, 611-0011, Japan

The dynamic Young's modulus (E'_L) and loss tangent (tan δ_L) along the grain, dynamic shear modulus (G'_L) and loss tangent (tan δ_S) in the vertical section, and density (ρ) of a hundred spruce wood specimens used for the soundboards of musical instruments were determined. The relative acoustic conversion efficiency (α, $\sqrt{E'_L/\rho}/\tan\delta_L$) and a ratio reflecting the anisotropy of wood (β, $(E'_L/G'_L)(\tan\delta_S/\tan\delta_L)$) were defined in order to evaluate the acoustic quality of wood along the grain. There was a positive correlation between α and β, and the variation in β was larger than that in α. It seemed logical to evaluate the acoustic quality of spruce wood by a measure of β. By using a cell wall model, those acoustic factors were expressed with the physical properties of the cell wall constituents. This model predicted that the essential requirement for an excellent soundboard is smaller fibril angle of the cell wall, which yields higher α and higher β. On the other hand, the effects of chemical treatments on the α and β of wood were clarified experimentally and analyzed theoretically. It was suggested that the α and β of wood cannot be improved at the same time by chemical treatment.

1. Introduction

Wood has been widely used as a material for the soundboards of musical instruments, such as violins and pianos. Since the quality of an instrument strongly depends on that of its wooden soundboard, much attention has been paid to the vibrational properties of wood. It is generally accepted that a high acoustic conversion efficiency and a large degree of anisotropy are required for an excellent soundboard [1–4]. The acoustic conversion efficiency is defined as the ratio of acoustic energy radiated from a beam to the vibration energy of the beam, and is proportional to $\sqrt{E'/\rho^3}/\tan\delta$, where E', ρ and $\tan\delta$ are the dynamic Young's modulus, density and mechanical loss tangent, respectively [5]. Actually, a high-grade wood specimen selected for the soundboard of an instrument has high E'/ρ and low $\tan\delta$, so consequently it possesses higher acoustic conversion efficiency than a low-grade one [1, 3]. On the other hand, the ratio of Young's modulus to the shear modulus (E'/G', G': dynamic shear modulus) of wood is higher than that of isotropic materials such as plastics and metals, owing to its anisotropic structure in the cell wall. As this ratio is related to the contribution of shear deformation in the flexural vibration of a beam, it determines the frequency response of a wooden soundboard [2, 3, 6–9]. It is well known that Sitka spruce wood, the preferred material for the soundboard of pianos, records a high E'/G' value, and that its damping in the high frequency range is greater than that of other wood species [7, 10]. Thus the E'/G' and related factors reflecting the anisotropy of wood may be also responsible for the quality of musical instruments [4, 11].

The relatively high acoustic conversion efficiency and E'/G' values of wood must be attributed to the fiber-matrix composite structure of its cell wall, as well as its porous cellular structure. In order to characterize the vibrational properties of wood, it is necessary to know the relationship between the microstructure of the wood cell wall and its vibrational properties. In this paper, the vibrational properties of wood along the grain are expressed by a simple mechanical model considering the microstructure of wood cell wall. This model enables us to understand the natural variation in acoustic factors of wood along the grain, and the effects of chemical treatments on the quality of soundboards.

2. Experimental procedure

2.1. Materials and treatment procedure

A hundred Sitka spruce (*Picea Sitchensis* Carr.) specimens obtained from material for the soundboard of a piano were used at a size of 3 mm (T, tangential direction) × 15 mm (R, radial direction) × 150 mm (L, longitudinal direction). The specimens were previously dried at 60°C under a vacuum for a day and weighed. After conditioning at 25°C and 60% relative humidity

(RH) for more than a month, their vibrational properties were measured. Next, thirty specimens with analogous vibrational properties were selected and divided into five groups. Of these, one group remained untreated and the other four were chemically treated by the following methods; Formalization (F), treated with formaldehyde with SO_2 at 120°C for 24 hours; Acetylation (A), treated in acetic anhydride at 120°C for 8 hours; Polyethylene glycol impregnation (P), soaked in 25% aqueous solution of polyethylene glycol (PEG, $M_w = 1000$) for a week; Hematoxylin impregnation (H) [12], soaked in 1.7% aqueous solution of hematoxylin for 12 days. After drying under atmospheric conditions and subsequent drying at 60°C under a vacuum for a few days, specimens were weighed. They were then conditioned at 25°C and 60% RH for more than a month, and their vibrational properties were determined again.

2.2. Measurement of vibrational properties

The measuring apparatus is schematically illustrated in Fig. 1. The dynamic Young's modulus (E'_L) and the loss tangent ($\tan\delta_L$) in the L direction were determined by using the free-free flexural vibration method [13]. A thin piece of 3 × 10 mm iron was attached to the end of a specimen. The specimen hung by silk threads was vibrated by a magnetic driver, and the amplitude of vibration was detected using microphone. The signal passed through the band pass filter was observed by FFT analyzer. After the resonance frequency of the specimen was determined, the magnetic driver was switched off and the decrement of vibration was recorded. The E'_L value of the specimen was calculated from the resonance frequency of the first mode, and its $\tan\delta_L$ value was calculated from the decay curve. The resonance frequency ranged from 600 to 850 Hz.

The dynamic shear modulus (G'_L) and loss tangent ($\tan\delta_S$) in the LR plane were measured by using the torsional vibration method [14]. The specimen was clamped near one end and hung vertically, and a weight made of iron was horizontally attached near the other end. A magnetic driver was faced to the end of the weight and a detector was faced to the opposite side of the other end. The rotatory vibration along the axis of the specimen was excited by the driver, and its amplitude was detected by a rock-in amplifier. The G'_L and $\tan\delta_S$ were calculated using the peak frequency and the half-value width in the resonance curve, respectively. The resonance frequency was in the range of 40 to 75 Hz. Since the dynamic properties of wood are almost independent of frequency in this temperature-frequency region [15], it is valid to use the values determined at different frequencies.

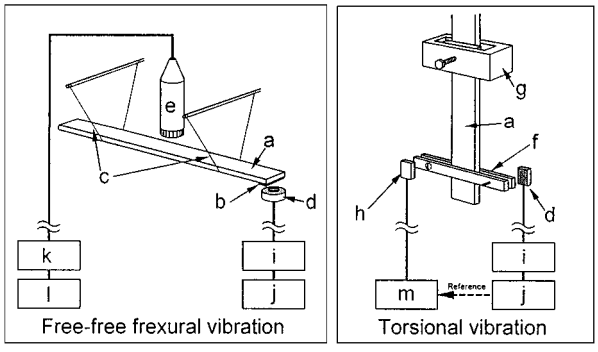

Figure 1 Schematic diagrams of the free-free flexural vibration apparatus and the torsional vibration apparatus. (a) wood specimen; (b) iron piece; (c) silk thread supporting the specimen; (d) magnetic driver; (e) microphone; (f) iron weight; (g) clamp; (h) detector; (i) amplifier; (j) generator; (k) band-pass filter; (l) FFT analyzer; (m) lock-in amplifier.

3. Results and discussion

3.1. Vibrational properties of natural wood

Fig. 2 shows the relationship between the $\tan\delta_L$ and E'_L/ρ for the spruce wood specimens. There was a high negative correlation between them. Such a relationship has been observed with many species of wood [16–18]. In the L direction, the E'_L/ρ and $\tan\delta_L$ of a specimen approximately represent the corresponding mean values of the wood cell wall. In practice, both quantities depends mainly on the mean microfibril angle of the cell wall (θ) as shown in Fig. 3, but very little on the density [17].

Fig. 4 represents the relationship between the ratio of loss tangent ($\tan\delta_S/\tan\delta_L$) and that of dynamic elastic moduli (E'_L/G'_L) for the spruce wood specimens. The positive correlation between them could be approximated by the following equation,

$$\frac{\tan\delta_S}{\tan\delta_L} = a\exp\left(\frac{bE'_L}{G'_L}\right).$$

Coefficients a and b were 1.00 and 0.57 for spruce wood specimens, and 1.00 and 0.61 for 101 different species. The regression curve for the spruce wood agreed well with that for other wood species. Owing to the anisotropic structure of the wood cell wall, its $\tan\delta_S/\tan\delta_L$ and E'_L/G'_L values were higher than those

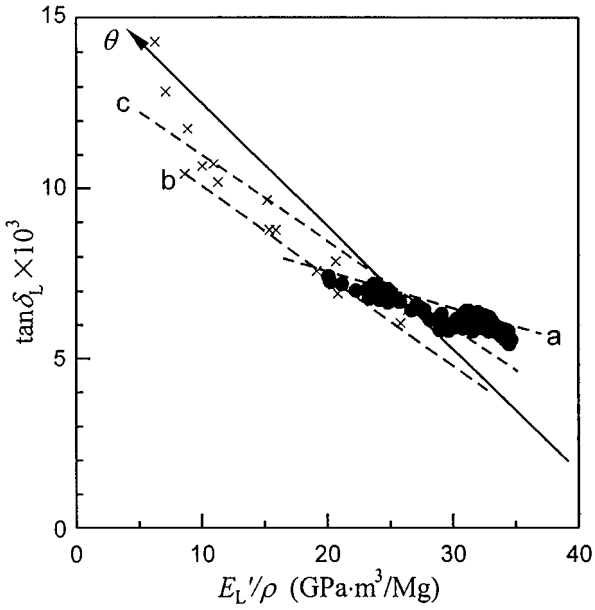

Figure 2 Relationship between $\tan\delta_L$ and E'_L/ρ of woods. ●, experimental values for spruce wood; (a) regression line for spruce wood; (b) regression line from 101 different wood species [18]; (c) regression line for Hinoki wood [17]; solid line, values calculated using a cell wall model.

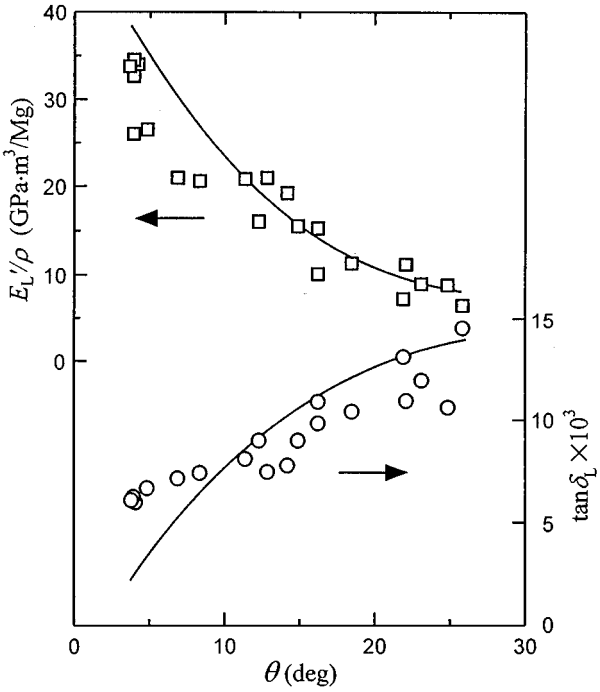

Figure 3 The E_L'/ρ (□) and $\tan\delta_L$ (○) for Hinoki wood plotted against the mean microfibril angle (θ) [17].

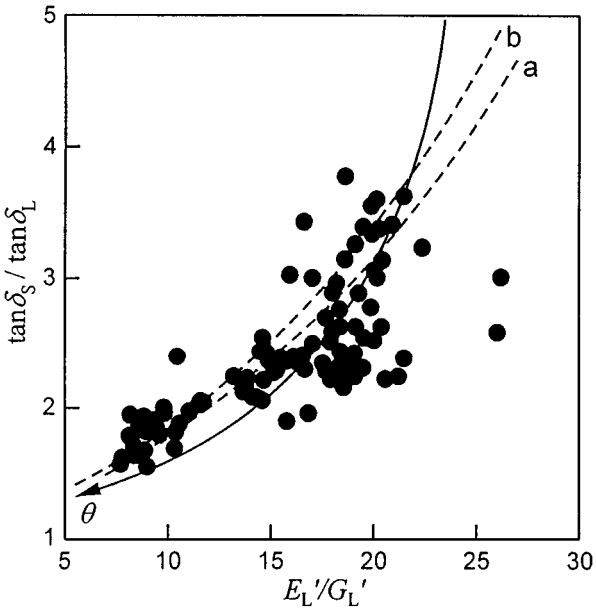

Figure 4 Relationship between $\tan\delta_S/\tan\delta_L$ and E_L'/G_L' of spruce wood. For keys, see Fig. 2.

of isotropic materials, which have values of approximately 1 for $\tan\delta_S/\tan\delta_L$ and 2–3 for E_L'/G_L'.

To evaluate the acoustic conversion efficiency of wood along the grain, a factor of $\sqrt{E_L'/\rho^3}/\tan\delta_L$ has been frequently used [3, 19–21]. However, this factor is inappropriate for the aim of this study because it depends strongly on ρ and does not reflect directly the microstructure of the wood cell wall. Thus we used another factor, $\alpha \equiv \sqrt{E_L'/\rho}/\tan\delta_L$, defined as relative acoustic conversion efficiency. It must be recalled that E_L'/ρ and $\tan\delta_L$ are independent of ρ and are equivalent to the corresponding values of the cell wall. In addition, the density of the cell wall is almost constant, consequently the α value of a wood specimen is proportional to the acoustic conversion efficiency of its cell wall.

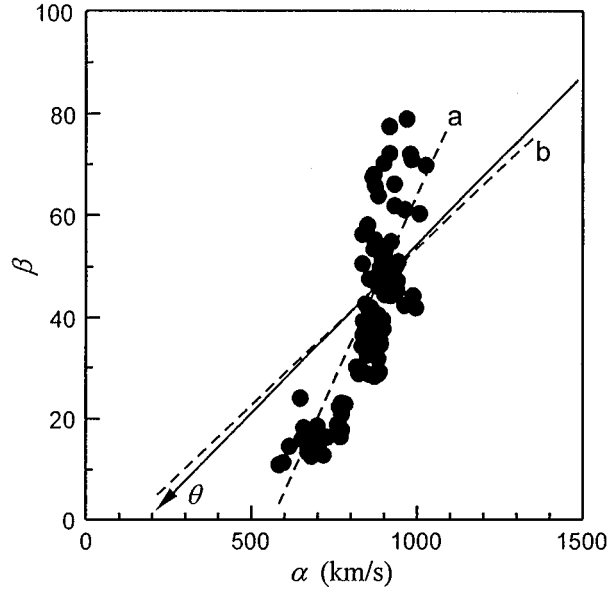

Figure 5 Relationship between β ($(E_L'/G_L')(\tan\delta_S/\tan\delta_L)$) and α ($\sqrt{E_L'/\rho}/\tan\delta_L$) of spruce wood. For keys, see Fig. 2.

The ratios E_L'/G_L' and $\tan\delta_S/\tan\delta_L$, reflecting the anisotropic nature of wood, affect the tone quality of wooden soundboards [2, 8, 9]. From the viewpoint of piano manufacturer, Nozaki and co-authors suggested that high E_L'/G_L' value of soundboard is important for the tone quality of the instrument [2]. This empirical law seems reasonable because the E_L'/G_L' value of wooden beam affects the frequency response of its flexural vibration [8]. Yano and Matsuhisa predicted that the higher E_L'/G_L' and higher $\tan\delta_S/\tan\delta_L$ values of wood specimen give larger acoustic loss at high frequencies, to reduce the high frequency sound radiation [9]. In fact, the high frequency sound radiation of coniferous wood specimen is relatively smaller than that of hardwood and metal [11]. The E_L'/G_L' and $\tan\delta_S/\tan\delta_L$ values are almost independent of ρ, and may reflect the anisotropic nature of the wood cell wall. As there is a positive correlation between E_L'/G_L' and $\tan\delta_S/\tan\delta_L$ irrespective of the wood species, $\beta \equiv (E_L'/G_L')(\tan\delta_S/\tan\delta_L)$ is here defined as an indication of tone quality of soundboard. Both α and β are good for evaluating the acoustic quality of wood because an excellent wooden soundboard has high E_L'/ρ, high E_L'/G_L', and low $\tan\delta_L$, i.e. high α and high β. Fig. 5 shows the relationship between β and α for the spruce wood specimens. A linear positive relation between them indicates that high α value of a spruce specimen is compatible with high β. A similar trend has been observed in many kinds of wood species [18]. However, it should be noted that the variation in the β of spruce wood is greater than that in the α. The β is recommended as a measure for selecting spruce wood specimens, when both the α and β values are required to be high.

3.2. Analysis using a cell wall model

As described above, the vibrational properties of wood vary widely even within a species. The vibrational properties discussed here are almost independent of the ρ of wood, and correspond to those of the wood cell wall. Therefore, the wide variation in the vibrational

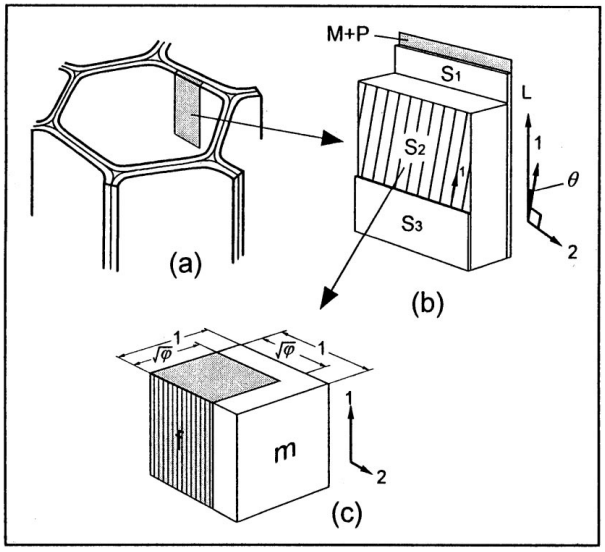

Figure 6 Schematic model of the wood cell wall for analogies.

properties of spruce wood specimens should be explained by that in their cell wall structure. Although many attempts have so far been made to relate the static elastic constants of wood specimen to those of the cell wall constituents, few investigations have dealt with the relations between the viscoelastic, i.e. vibrational properties of wood and its microstructure. In this section, the vibrational properties of wood are expressed by using a simple cell wall model [12, 23]. This model provides us with a clear understanding of the wide variation in the vibrational properties of natural wood.

Fig. 6 is a schematic representation of the wood cell wall. The cell wall has a multi-layered structure composed of middle (M), primary (P) and secondary (S_1, S_2 and S_3) layers as shown in Fig. 6a and b. At the macromolecular level (1 to 100 nm), each layer can be schematically described as a two-phase composite of elastic fibrils consisting of cellulose and a part of hemicellulose (f), and a viscoelastic matrix consisting of lignin and the remaining part of hemicellulose (m) as illustrated in Fig. 6c. In this simplified modeling, the amorphous matrix can be regarded as an isotropic substance although the lignin shows some anisotropy in the cell wall [24]. In a layer, the fibrils embedded in the matrix are oriented in a direction (the 1 direction) at an angle (θ) to the L direction. The Young's modulus of a layer in the L direction ($E_{\mathrm{L}}^{\mathrm{w}}$) and shear modulus in its plane ($G_{\mathrm{L}}^{\mathrm{w}}$) are expressed by

$$E_{\mathrm{L}}^{\mathrm{w}} = \left[\frac{\cos^4\theta}{E_1^{\mathrm{w}}} + \left(\frac{1}{G_{12}^{\mathrm{w}}} - \frac{2\mu_{12}}{E_1^{\mathrm{w}}} \right) \sin^2\theta \cos^2\theta + \frac{\sin^4\theta}{E_2^{\mathrm{w}}} \right]^{-1} \tag{1}$$

and

$$G_{\mathrm{L}}^{\mathrm{w}} = \left[\frac{\sin^2 2\theta}{E_1^{\mathrm{w}}}(1 + 2\mu_{12}) + \frac{\sin^2 2\theta}{E_2^{\mathrm{w}}} + \frac{\cos^2 2\theta}{G_{12}^{\mathrm{w}}} \right]^{-1}, \tag{2}$$

where E_1^{w} and E_2^{w} are the Young's modulus of a layer in the 1 and 2 directions, respectively, G_{12}^{w} the shear modulus of a layer in the 1–2 plane, and μ_{12} the Poisson's ratio. The 2 direction is perpendicular to the fibril axis. When the θ is small enough to ensure $\sin^4\theta \approx 0$, and μ_{12} is small enough to ignore $2\mu_{12}/E_1^{\mathrm{w}}$ compared to $1/G_{12}^{\mathrm{w}}$ and $(1 + 2\mu_{12})/E_1^{\mathrm{w}}$ to $1/E_2^{\mathrm{w}}$ [25], Equations 1 and 2 are approximately expressed by

$$E_{\mathrm{L}}^{\mathrm{w}} \approx \left(\frac{\cos^4\theta}{E_1^{\mathrm{w}}} + \frac{\sin^2\theta\ \cos^2\theta}{G_{12}^{\mathrm{w}}} \right)^{-1} \tag{3}$$

and

$$G_{\mathrm{L}}^{\mathrm{w}} \approx \left(\frac{\sin^2 2\theta}{E_2^{\mathrm{w}}} + \frac{\cos^2 2\theta}{G_{12}^{\mathrm{w}}} \right)^{-1} \tag{4}$$

In linear viscoelastic media, it is safe to replace static rigidities or compliance by their corresponding complex values, and imaginary parts are always considered as much smaller than the real parts in the time-temperature domain calculated here for wood, so that the complex Young's modulus of a layer in the L direction, $E_{\mathrm{L}}^{\mathrm{w}*}(=E_{\mathrm{L}}^{\mathrm{w}\prime} + iE_{\mathrm{L}}^{\mathrm{w}\prime\prime})$, and the complex shear modulus in a layer, $G_{\mathrm{L}}^{\mathrm{w}*}(=G_{\mathrm{L}}^{\mathrm{w}\prime} + iG_{\mathrm{L}}^{\mathrm{w}\prime\prime})$, are related to the quantities, $E_1^{\mathrm{w}*}(=E_1^{\mathrm{w}\prime} + iE_1^{\mathrm{w}\prime\prime})$, $E_2^{\mathrm{w}*}(=E_2^{\mathrm{w}\prime} + iE_2^{\mathrm{w}\prime\prime})$ and $G_{12}^{\mathrm{w}*}(=G_{12}^{\mathrm{w}\prime} + iG_{12}^{\mathrm{w}\prime\prime})$, by

$$\begin{aligned} E_{\mathrm{L}}^{\mathrm{w}*} &\approx \left(\frac{\cos^4\theta}{E_1^{\mathrm{w}*}} + \frac{\sin^2\theta\cos^2\theta}{G_{12}^{\mathrm{w}\prime}} \right)^{-1} \\ &\approx \left[\frac{\cos^4\theta}{E_1^{\mathrm{w}\prime}} + \frac{\sin^2\theta\cos^2\theta}{G_{12}^{\mathrm{w}\prime}} - i\left(\frac{E_1^{\mathrm{w}\prime\prime}\cos^4\theta}{E_1^{\mathrm{w}\prime 2}} + \frac{G_{12}^{\mathrm{w}\prime\prime}\sin^2\theta\cos^2\theta}{G_{12}^{\mathrm{w}\prime 2}} \right) \right]^{-1}, \end{aligned} \tag{5}$$

and

$$\begin{aligned} G_{\mathrm{L}}^{\mathrm{w}*} &\approx \left(\frac{\sin^2 2\theta}{E_2^{\mathrm{w}*}} + \frac{\cos^2 2\theta}{G_{12}^{\mathrm{w}*}} \right)^{-1} \\ &\approx \left[\frac{\sin^2 2\theta}{E_2^{\mathrm{w}\prime}} + \frac{\cos^2 2\theta}{G_{12}^{\mathrm{w}\prime}} - i\left(\frac{E_2^{\mathrm{w}\prime\prime}\sin^2 2\theta}{E_2^{\mathrm{w}\prime 2}} + \frac{G_{12}^{\mathrm{w}\prime\prime}\cos^2 2\theta}{G_{12}^{\mathrm{w}\prime 2}} \right) \right]^{-1}. \end{aligned} \tag{6}$$

Therefore, the real and imaginary parts of $E_{\mathrm{L}}^{\mathrm{w}*}$ and $G_{\mathrm{L}}^{\mathrm{w}*}$ are

$$E_{\mathrm{L}}^{\mathrm{w}\prime} \approx \left(\frac{\cos^4\theta}{E_1^{\mathrm{w}\prime}} + \frac{\sin^2\theta\cos^2\theta}{G_{12}^{\mathrm{w}\prime}} \right)^{-1}$$

and

$$E_{\mathrm{L}}^{\mathrm{w}\prime\prime} \approx \left(\frac{E_1^{\mathrm{w}\prime\prime}\cos^4\theta}{E_1^{\mathrm{w}\prime 2}} + \frac{G_{12}^{\mathrm{w}\prime\prime}\sin^2\theta\cos^2\theta}{G_{12}^{\mathrm{w}\prime 2}} \right) \times \left(\frac{\cos^4\theta}{E_1^{\mathrm{w}\prime}} + \frac{\sin^2\theta\cos^2\theta}{G_{12}^{\mathrm{w}\prime}} \right)^{-2}, \tag{7}$$

$$G_{\mathrm{L}}^{\mathrm{w}\prime} \approx \left(\frac{\sin^2 2\theta}{E_2^{\mathrm{w}\prime}} + \frac{\cos^2 2\theta}{G_{12}^{\mathrm{w}\prime}} \right)^{-1}$$

and

$$G_{\mathrm{L}}^{\mathrm{w}\prime\prime} \approx \left(\frac{E_2^{\mathrm{w}\prime\prime} \sin^2 2\theta}{E_2^{\mathrm{w}\prime 2}} + \frac{G_{12}^{\mathrm{w}\prime\prime} \cos^2 2\theta}{G_{12}^{\mathrm{w}\prime 2}} \right) \times \left(\frac{\sin^2 2\theta}{E_2^{\mathrm{w}\prime}} + \frac{\cos^2 2\theta}{G_{12}^{\mathrm{w}\prime}} \right)^{-2}. \quad (8)$$

Next, those equations are related to local quantities of the cell wall constituents. As the fibrils and matrix are almost in parallel in the 1 direction, the complex Young's modulus $E_1^{\mathrm{w}*}$ is given by

$$E_1^{\mathrm{w}*} = \varphi E_1^{\mathrm{f}} + (1-\varphi)(E_{\mathrm{m}}' + i E_{\mathrm{m}}'').$$

Therefore,

$$E_1^{\mathrm{w}\prime} = \varphi E_1^{\mathrm{f}} + (1-\varphi) E_{\mathrm{m}}' \quad \text{and} \quad E_1^{\mathrm{w}\prime\prime} = (1-\varphi) E_{\mathrm{m}}'', \quad (9)$$

where E_1^{f} is the Young's modulus of fibrils in the 1 direction, E_{m}^* ($=E_{\mathrm{m}}^* + i E_{\mathrm{m}}''$) the complex Young's modulus of matrix, and φ the volume fraction of fibrils.

The fibrils with a square cross section are embedded in matrix as illustrated in Fig. 6c, so that fibrils and matrix are aligned partly in series and partly to the force in the 2 direction. According to the law of mixtures, the complex Young's modulus $E_2^{\mathrm{w}*}$ is given by

$$\begin{aligned} E_2^{\mathrm{w}*} &= (1-\sqrt{\varphi}) E_{\mathrm{m}}^* + \sqrt{\varphi} \left(\frac{\sqrt{\varphi}}{E_2^{\mathrm{f}}} + \frac{1-\sqrt{\varphi}}{E_{\mathrm{m}}^*} \right)^{-1} \\ &= (1-\sqrt{\varphi})\left(E_{\mathrm{m}}' + i E_{\mathrm{m}}''\right) \\ &\quad + \sqrt{\varphi} E_2^{\mathrm{f}} \frac{E_{\mathrm{m}}' + i E_{\mathrm{m}}''}{\sqrt{\varphi} E_{\mathrm{m}}' + (1-\sqrt{\varphi}) E_2^{\mathrm{f}} + i\sqrt{\varphi} E_{\mathrm{m}}''}, \end{aligned}$$

where E_2^{f} is the Young's modulus of fibrils in the 2 direction. By assuming $E_{\mathrm{m}}'^2 \gg E_{\mathrm{m}}''^2$,

$$E_2^{\mathrm{w}*} \approx E_{\mathrm{m}}' \left(1 - \sqrt{\varphi} + \frac{\sqrt{\varphi} E_2^{\mathrm{f}}}{A}\right) + i E_{\mathrm{m}}''(1-\sqrt{\varphi}) \left(1 + \sqrt{\varphi} \frac{E_2^{\mathrm{f}2}}{A^2}\right),$$

where $A = \sqrt{\varphi} E_{\mathrm{m}}' + (1-\sqrt{\varphi}) E_2^{\mathrm{f}}$.

The real and imaginary part of $E_2^{\mathrm{w}*}$ are thus given by

$$E_2^{\mathrm{w}\prime} \approx E_{\mathrm{m}}' \left(1 - \sqrt{\varphi} + \frac{\sqrt{\varphi} E_2^{\mathrm{f}}}{A}\right)$$

and

$$E_2^{\mathrm{w}\prime\prime} \approx E_{\mathrm{m}}''(1-\sqrt{\varphi}) \left(1 + \sqrt{\varphi} + \sqrt{\varphi} \frac{E_2^{\mathrm{f}2}}{A^2}\right). \quad (10)$$

The analogous approximation gives the real and imaginary part of $G_{12}^{\mathrm{w}*}$ as

$$G_{12}^{\mathrm{w}\prime} \approx G_{\mathrm{m}}' \left(1 - \sqrt{\varphi} + \frac{\sqrt{\varphi} G_{12}^{\mathrm{f}}}{B}\right)$$

and

$$G_{12}^{\mathrm{w}\prime\prime} \approx G_{\mathrm{m}}''(1-\sqrt{\varphi}) \left(1 + \sqrt{\varphi} \frac{G_{12}^{\mathrm{f}2}}{B^2}\right), \quad (11)$$

where $B = \sqrt{\varphi} G_{\mathrm{m}}' + (1-\sqrt{\varphi}) G_{12}^{\mathrm{f}}$, G_{12}^{f} is the shear modulus of fibrils in the 1–2 plane, and G_{m}' and G_{m}'' are the real and imaginary part of the complex shear modulus of matrix, respectively. The vibrational properties of a layer, $E_{\mathrm{L}}^{\mathrm{w}\prime}$, $E_{\mathrm{L}}^{\mathrm{w}\prime\prime}$, $G_{\mathrm{L}}^{\mathrm{w}\prime}$ and $G_{\mathrm{L}}^{\mathrm{w}\prime\prime}$ can be obtained by combining the Equations 7–11.

In the L direction, the mechanical properties of the cell wall are mainly governed by those of the thickest S_2 layer. Thus, the vibrational properties of wood are expressed by

$$\frac{E_{\mathrm{L}}'}{\rho} = \frac{v E_{\mathrm{L}}^{\mathrm{w}\prime}}{\rho_{\mathrm{w}}}, \quad (12)$$

$$\tan\delta_{\mathrm{L}} = \frac{E_{\mathrm{L}}^{\mathrm{w}\prime\prime}}{E_{\mathrm{L}}^{\mathrm{w}\prime}}, \quad (13)$$

$$\frac{E_{\mathrm{L}}'}{G_{\mathrm{L}}'} = \frac{E_{\mathrm{L}}^{\mathrm{w}\prime}}{G_{\mathrm{L}}^{\mathrm{w}\prime}} \quad (14)$$

and

$$\frac{\tan\delta_{\mathrm{S}}}{\tan\delta_{\mathrm{L}}} = \frac{E_{\mathrm{L}}^{\mathrm{w}\prime}}{E_{\mathrm{L}}^{\mathrm{w}\prime\prime}} \cdot \frac{G_{\mathrm{L}}^{\mathrm{w}\prime\prime}}{G_{\mathrm{L}}^{\mathrm{w}\prime}}, \quad (15)$$

where v is the volume fraction of the S_2 layer in the cell wall, and ρ_{w} the density of the cell wall.

Experimental values of 0.84, 0.531, 1.43 and 134 GPa were adopted for v, φ, ρ_{w} and E_1^{f} [26, 27]. For E_2^{f} and G_{12}^{f}, the estimated values of 27.2 GPa and 4.4 GPa were used [25]. The dynamic elastic moduli E_{m}' and G_{m}' of matrix were substituted by the corresponding static elastic moduli of lignin [28], the main constituent of matrix. As it is known that the fibril angle of the S_2 layer varies widely, θ was varied from 5° to 30° in this calculation. There is regrettably no information about the loss factor of the matrix. In this calculation, a hypothetical value of 0.025 was used for $\tan\delta_{\mathrm{m}}$ ($=E_{\mathrm{m}}''/E_{\mathrm{m}}' = G_{\mathrm{m}}''/G_{\mathrm{m}}'$), taking into consideration the loss tangents of phenol and isocyanate resins and some natural resins consisting of catechol derivatives [29, 30]. The parameters for the calculation are summarized in Table I, and the calculated values are compared to the corresponding experimental values reported in Figs 2 to 5. Considering the simplicity of the model, agreement with the experimental data was very good.

This model clearly predicts that θ is the most important factor determining the vibrational properties of wood along the grain. With decreasing θ, the E_{L}'/ρ increases and the $\tan\delta_{\mathrm{L}}$ decreases, while the G_{L}'/ρ and

TABLE I Parameters used for the calculation

		Fibrils			Matrix		
v	φ	E_1^f (GPa)	E_2^f (GPa)	G_{12}^f (GPa)	E'_m (GPa)	G'_m (GPa)	$\tan\delta_m$
0.84	0.531	134	27.2	4.4	4	1.5	0.025

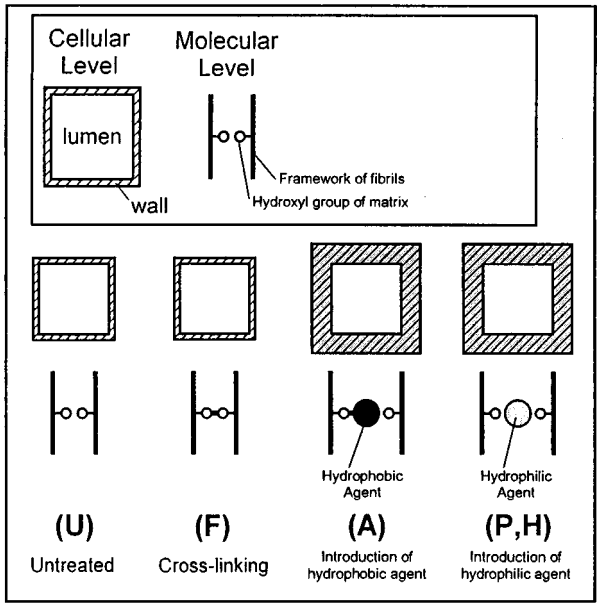

Figure 7 Structural changes of wood at the cellular and molecular levels due to formalization (F), acetylation (A), polyethylene glycol impregnation (P) and hematoxylin impregnation (H), compared with untreated (U) wood.

$\tan\delta_S$ remain almost unchanged, consequently both the α and β increased. The smaller θ is essential for an excellent wooden soundboard, when a higher α and higher β values are required.

3.3. Effects of chemical treatment on the vibrational properties of natural wood

Various chemical treatments have been developed for the improvement of wooden soundboards. In most cases, such treatment increases the E'/ρ and reduces the $\tan\delta$ of wood, to enhance its acoustic conversion efficiency [3, 19–21]. In addition, the dimensional and creep stability of wood is improved by some treatments [31]. However, few studies have dealt with the effects of chemical treatments on the E'_L/G'_L and $\tan\delta_S/\tan\delta_L$ values of wood, being important for the tone quality of instruments. In this section, the effects of some typical chemical treatments on the vibrational properties of wood are clarified experimentally and analyzed theoretically by using the cell wall model.

Fig. 7 illustrates schematically the structural changes of the cell wall due to the typical treatments employed in this study [31]. The treatments discussed here exclude any radical treatment resulting in destruction of the cellular structure or fiber-matrix composite structure in the cell wall. Formalization (F) is a reaction involving the formation of oxymethylene bridges between the hydroxyl groups of the matrix by formaldehyde. In acetylation (A), hydrophilic hydroxyl groups of the matrix are substituted with hydrophobic acetyl groups. The introduction of bulky agent induces remarkable swelling of the wood cell wall. In addition, the hydrophobic nature of acetyl groups reduces the hygroscopicity of wood. Polyethylene glycol impregnation (P) gives rise to remarkable swelling of wood due to the penetration of PEG molecules into the cell wall. Hematoxylin impregnation (H) is a treatment recently developed, and is similar to P treatment in respect to the treating process. By this treatment, water-soluble hematoxylin is introduced into the cell wall causing slight swelling.

Table II lists the weight percent gain (WPG) and changes of vibrational properties due to treatments. Figs 8 to 10 show the relationships of E'_L/ρ vs. $\tan\delta_L$, E'_L/G'_L vs. $\tan\delta_S/\tan\delta_L$ and α vs. β for the untreated

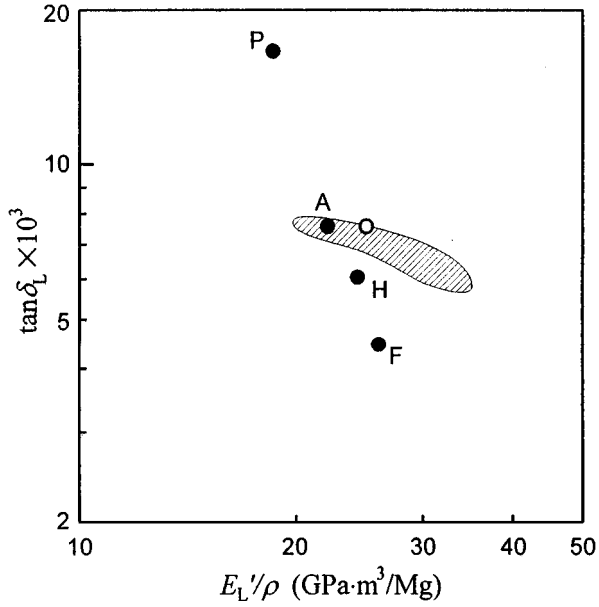

Figure 8 E'_L/ρ and $\tan\delta_L$ of untreated (○) and treated (●) spruce wood specimens. For keys, see Fig. 7.

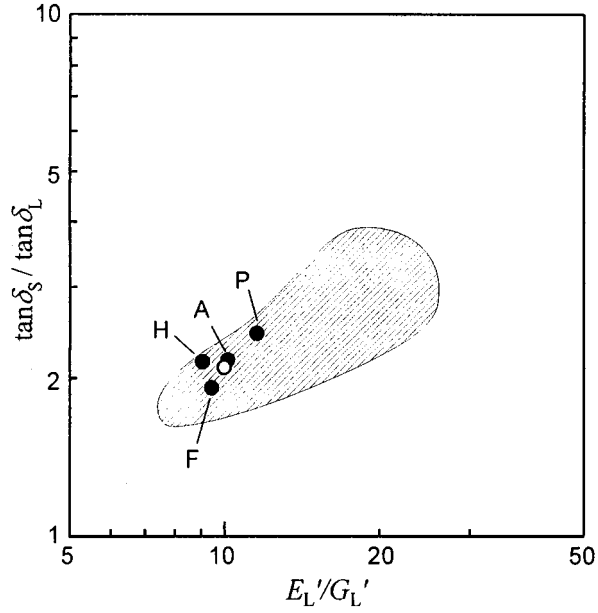

Figure 9 E'_L/G'_L and $\tan\delta_S/\tan\delta_L$ of untreated (○) and treated (●) spruce wood specimens. For keys, see Fig. 7.

TABLE II Vibrational properties of chemically treated spruce woods

	WPG (%)	MC (%)	ρ (Mg/m^3)	E'_L (GPa)	E'_L/ρ (GPA · m^3/Mg)	$\tan\delta_L$	G'_L (GPa)	G'_L/ρ (GPa · m^3/Mg)	$\tan\delta_S$	E'_L/G'_L	$\tan\delta_S/\tan\delta_L$	α (km/s)	β
U		−8.84	0.409	−10.3	−25.1	−0.0076	−1.03	−2.52	−0.016	−10.07	−2.06	−665	−20.9
F		−2.94	0.410	−10.8	−26.3	−0.0044	−1.15	−2.81	−0.009	−9.52	−1.90	−1121	−18.4
A		−4.27	0.442	−9.9	−22.3	−0.0075	−0.97	−2.19	−0.016	−10.21	−2.14	−634	−22.0
H		−8.75	0.423	−10.4	−24.5	−0.0060	−1.16	−2.75	−0.013	−9.14	−2.13	−812	−19.8
P		−7.27	0.488	−9.1	−18.7	−0.0165	−0.77	−1.57	−0.038	−11.58	−2.42	−279	−27.7
Changes (%)													
F	5.6	−66.7	0.4	−4.8	−4.4	−41.3	−11.9	−11.6	−42.2	−5.5	−7.9	−68.6	−11.9
A	18.4	−51.8	8.1	−4.2	−11.3	−1.2	−5.6	−13.1	−2.8	−1.5	−3.8	−4.7	−5.2
H	5.8	−1.1	3.5	−0.9	−2.5	−20.2	−13.0	−9.1	−15.3	−9.2	−3.5	−22.2	−5.2
P	31.6	−17.7	19.4	−11.4	−25.7	−118.4	−24.7	−37.9	−145.7	−15.1	−17.4	−58.1	−32.8

WPG, Weight percent gain due to treatment; MC, moisture content at 25°C and 60%RH based on the weight of dry specimen; U, untreated; F, formalized; A, acetylated; H, impregnated with hematoxylin; P, impregnated with polyethylene glycol.

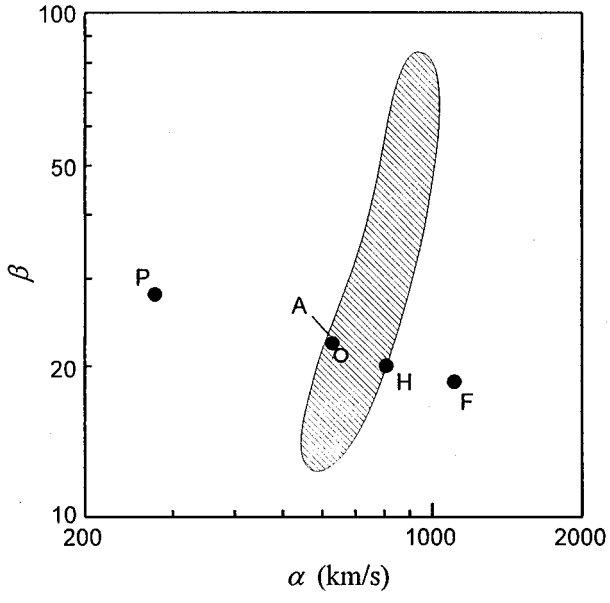

Figure 10 The α and β of untreated (○) and treated (●) spruce wood specimens. For keys, see Fig. 7.

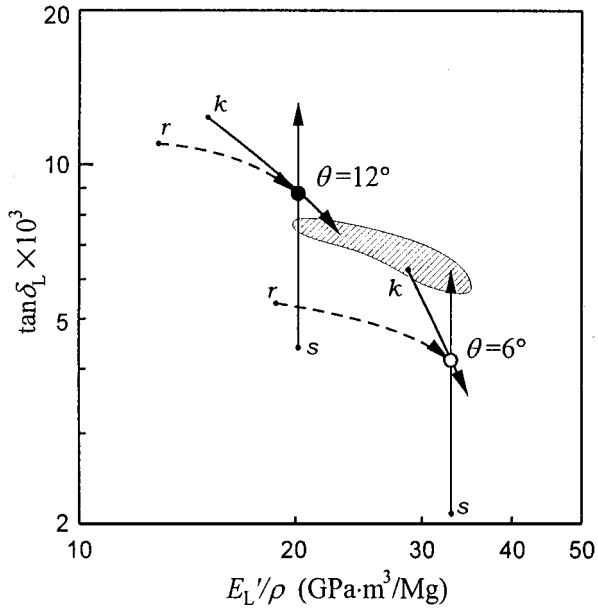

Figure 11 Calculated values of E'_L/ρ and $\tan\delta$ for untreated ($k = s = r = 1$) wood at a θ of 6° (○) and 12° (●), and the range of calculated value for treated wood. k, changes of matrix elasticity ranging from 0.5 to 1.5; s, change of loss tangent of matrix ranging from 0.5 to 1.5; r, change of fibril fraction from 0.5 to 1.0.

and chemically treated spruce woods, respectively. The variations in the corresponding experimental values for the untreated spruce wood specimens are shown by the hatched area on each graph. By the F treatment, the E'_L/ρ increased and $\tan\delta_L$ decreased whereas E'_L/G'_L and $\tan\delta_S/\tan\delta_L$ decreased, consequently, the β decreased slightly while α increased remarkably. The effects of H treatment were similar to those of F treatment, except for a slight reduction of E'_L/ρ. With the A treatment, the changes in vibrational properties were relatively small. The P treatment induced remarkable increase of $\tan\delta_L$ and reduction of E'_L/ρ while it enhanced E'_L/G'_L and $\tan\delta_S/\tan\delta_L$ slightly, so that it reduced α whereas it increased β slightly. Generally, chemical treatment affects the α rather than β of wood, and the changes in α and β due to treatment show a reversed trend.

Now the effects of chemical treatment are generalized by using the cell wall model. As the θ of a natural wood specimen is unchanged by treatment, the θ is fixed at 6° and 12° in this simulation, representative of high-grade and low-grade wood specimens, respectively. The effects of treatments on the volume fraction of fibrils (φ) and the viscoelastic properties of matrix (E'_m, G'_m, $\tan\delta_m$) can be expressed by

$$r = \frac{\varphi(\text{treated})}{\varphi(\text{untreated})},$$

$$k = \frac{E'_m\,(\text{treated})}{E'_m\,(\text{untreated})} = \frac{G'_m\,(\text{treated})}{G'_m\,(\text{untreated})}$$

$$\text{and } s = \frac{\tan\delta_m\,(\text{treated})}{\tan\delta_m\,(\text{untreated})},$$

where r, k and s are constants representing the structural changes due to the treatments. In most cases, chemical treatment induces swelling of the matrix to reduce r, so that r varies from 0.5 to 1.0. On the other hand, k and s varies from 0.5 to 1.5 in this simulation. Figs 11 to 13 exhibit the calculated values with respect to the relations of E'_L/ρ vs. $\tan\delta_L$, E'_L/G'_L vs. $\tan\delta_S/\tan\delta_L$ and α vs. β, respectively. Here we explain the effects of all chemical treatments shown in Figs 8 to 10 by the changes of r, k and s exhibited in Figs 11 to 13. The F treatment

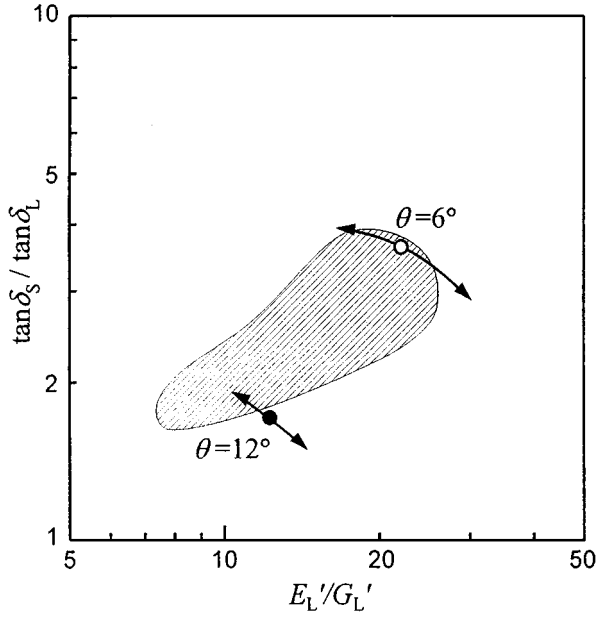

Figure 12 Calculated values of E_L'/G_L' and $\tan\delta_S/\tan\delta_L$. For keys, see Fig. 11.

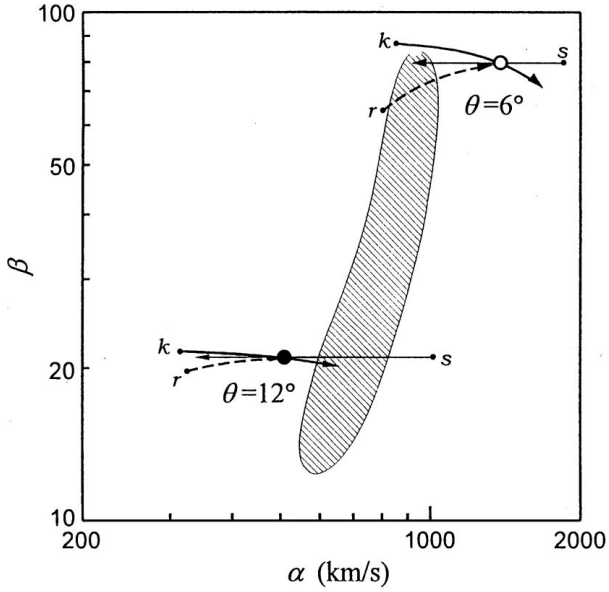

Figure 13 Calculated values of α and β. For keys, see Fig. 11.

involving the formation of cross-linking reduces the mobility of matrix molecules with little swelling ($r \approx 1$, $k > 1, s < 1$), resulting in the increase of E_L'/ρ and a remarkable reduction of $\tan\delta_L$. The effects of the H treatment are similar to those of the F treatment, probably because of steric hindrance of the bulky hematoxylin molecules penetrating the matrix or the formation of tight hydrogen bonds between the hematoxylin and the adjacent matrix molecules ($k > 1, s < 1$). The slight reduction of E_L'/ρ due to this treatment can be explained by the swelling effect of hematoxylin, involving the reduction of $r(r < 1)$. By the A treatment, hydrophobic acetyl groups impose the steric hindrance of matrix molecules to reduce their mobility ($k > 1, s < 1$), while inducing a remarkable swelling of matrix ($r < 1$). As these effects might be compensated, the changes of vibrational properties due to the A treatment are smaller than those of other treatments. The flexible hydrophilic PEG molecules introduced by the P treatment cause remarkable swelling of matrix ($r < 1$) and increase of matrix mobility ($k < 1, s > 1$). These are the reasons for the reduction of E_L'/ρ and increase of $\tan\delta_L$.

As we need not improve naturally high-graded specimens, the aim of the chemical treatment is to convert low-grade wood to high-grade wood. However, both the experimental and simulated results suggest that the β of wood can not be improved by chemical treatment though the α is remarkably affected by such treatment (Fig. 13). This fact indicates that the low-grade wood cannot be converted to the high-grade one by chemical treatment.

Yano and co-authors claimed that the acoustic quality of wooden soundboards could be much improved by chemical treatments involving the remarkable increase of acoustic conversion efficiency [3, 19–21]. However, most of their data indicates that the anisotropy of wood is reduced by those treatments. It seems strange that they did not mention the reduction of anisotropy due to treatments, while he emphasized the importance of anisotropy for the tone quality of soundboards [3].

The acoustic quality of wood strongly depends on the fibril angle of the cell wall, which is determined over a long period of natural growth and remains unaffected by treatment. In order to obtain a high-quality wood specimen for the soundboards of musical instruments, it is best not to modify the natural balance in the vibrational properties of wood, but to select a wood specimen of naturally high quality.

4. Conclusions

The vibrational properties of spruce wood used for the soundboards of musical instruments were discussed with respect to their relative acoustic conversion efficiency (α, $\sqrt{E_L'/\rho}/\tan\delta_L$) and a ratio reflecting anisotropic nature of wood (β, (E_L'/G_L') $(\tan\delta_S/\tan\delta_L)$). There was a good positive correlation between α and β values, and the variation in β was larger than that in α. Thus β is recommended for evaluating the acoustic quality of wooden soundboards. By using a simple cell wall model, these acoustic factors were well expressed with the viscoelastic parameters of the cell wall constituents. This model predicted that the essential requirement for an excellent soundboard is smaller fibril angle of the cell wall, which yields higher α and higher β. On the other hand, it was confirmed experimentally and theoretically that the α and β of wood cannot be improved at the same time by chemical treatment.

Acknowledgements

The authors are indebted to K. Minato, Assistant Professor of Kyoto University, for his kind assistance in the chemical treatments of wood specimens. The authors also express their gratitude to S. Yamamoto, YAMAHA Co. Ltd., who kindly provided spruce wood specimens.

References

1. M. NORIMOTO, *Mokuzai Gakkaishi* **28** (1982) 407.
2. K. NOZAKI, H. HAYASHIDA and T. YAMADA, *J. Jpn. Soc. Mech. Eng.* **91** (1988) 653.
3. H. YANO, H. KAJITA and K. MINATO, *J. Acoust. Soc. Am.* **96** (1994) 3380.

4. T. ONO, *J. Acoust. Soc. Jpn.(E)* **17** (1996) 183.
5. B. A. YANKOVSKII, *Sov. Phys. Acoust.* **13** (1967) 125.
6. R. F. S. HEARMON, *Br. J. Appl. Phys.* **9** (1958) 381.
7. T. ONO and A. KATAOKA, *Mokuzai Gakkaishi* **25** (1979) 535.
8. T. NAKAO, T. OKANO and I. ASANO, *J. Appl. Mech.* **52** (1985) 728.
9. H. YANO and H. MATSUHISA, *Scientific Reports of the Kyoto Pref. Univ.* **43** (1991) 24.
10. H. MEINEL, *J. Acoust. Soc. Am.* **29** (1957) 817.
11. H. YANO, *Mokuzai Kogyo* **48** (1993) 542.
12. K. MINATO, K. SAKAI, M. MATSUNAGA and F. NAKATSUBO, *Mokuzai Gakkaishi* **43** (1997) 1035.
13. R. F. S. HEARMON, *J. Appl. Mech.* **26** (1959) 537.
14. T. ONO, *Mokuzai Gakkaishi* **26** (1980) 139.
15. M. TONOSAKI, T. OKANO and I. ASANO, *ibid.* **29** (1983) 547.
16. T. ONO and M. NORIMOTO, *Jpn. J. Appl. Phys.* **24** (1985) 960.
17. M. NORIMOTO, F. TANAKA, T. OHOGAMA and R. IKIMUNE, *Wood Res. Tech. Notes* **22** (1986) 53.
18. H. AIZAWA, E. OBATAYA, T. ONO and M. NORIMOTO, *Wood Research* **85** (1998) 110.
19. H. YANO and K. MINATO, *J. Acoust. Soc. Am.* **92** (1992) 1222.
20. *Idem., Wood Sci. Technol.* **27** (1993) 287.
21. H. YANO, Y. FURUTA and H. NAKAGAWA, *J. Acoust. Soc. Am.* **101** (1997) 1112.
22. E. OBATAYA, J. GRIL and M. NORIMOTO, *Polymer* **39** (1998) 3059.
23. M. SUGIYAMA, E. OBATAYA and M. NORIMOTO, *J. Materials Sci.* **33** (1998) 3505.
24. R. H. ATALLA and U. P. AGARWAL, *Science* **227** (1985) 636.
25. R. E. MARK, "Cell Wall Mechanics of Tracheids" (Yale Univ. Press, New Haven, 1967), p. 119, 227.
26. T. OHOGAMA, M. MASUDA and T. YAMADA, *Jpn. J. Material. Sci.* **26** (1977) 433.
27. I. SAKURADA, Y. NUKUSHINA and T. ITO, *J. Polym. Sci.* **57** (1962) 651.
28. W. J. COUSINS, *Wood Sci. Tech.* **10** (1976) 9.
29. K. UMEMURA, A. TAKAHASHI and S. KAWAI, *J. Wood Sci.* **44** (1998) 204.
30. E. OBATAYA, Y. OHNO and M. NORIMOTO, *Mokuzai Gakkaishi* **44** (1998) 89.
31. M. NORIMOTO, J. GRIL and R. M. ROWELL, *Wood Fiber Sci.* **24** (1992) 25.

Received 6 May
and accepted 15 December 1999